†Work partially supported by the National Science Foundation under Grant No. GP7907X.

[1]See the reviews in *Advances in Chemical Physics*, edited by I. Prigogine and S. Rice (Interscience, New York, 1969), Vol. 14.

[2]J. Goldstone, Proc. Roy. Soc. (London) A239, 267 (1957); H. P. Kelly, in *Advances in Theoretical Physics*, edited by K. A. Brueckner (Academic, New York, 1968), Vol. 2, p. 75.

[3]John H. Miller and H. P. Kelly, Phys. Rev. A 3, 578 (1971).

[4]T. Lee, N. C. Dutta, and T. P. Das, Phys. Rev. A 4, 1410 (1971).

[5]N. C. Dutta, C. Matsubara, R. T. Pu, and T. P. Das, Phys. Rev. 177, 33 (1969).

[6]R. K. Nesbet, T. L. Barr, and E. R. Davidson, Chem. Phys. Letters 4, 203 (1969).

[7]Jimmy W. Viers, Frank E. Harris, and Henry F. Schaefer, Phys. Rev. A 1, 24 (1970).

[8]Terry L. Barr and Ernest R. Davidson, Phys. Rev. A 1, 644 (1970).

[9]Carlos F. Bunge and Eduardo M. A. Peixoto, Phys. Rev. A 1, 1277 (1970).

[10]Attention is drawn to the work by O. Sinanoğlu and coworkers who examine the magnitude of many-electron correlations as compared to the pair correlation. See, for example, O. Sinanoğlu, J. Chem. Phys. 36, 706 (1962); 41, 2683 (1964); O. Sinanoğlu and I. Öksüz, Phys. Rev. Letters 21, 507 (1968).

[11]R. K. Nesbet, Phys. Rev. 175, 2 (1968).

[12]Oscar R. Platas and Henry F. Schaefer III, Phys. Rev. A 4, 33 (1971).

[13]The Hartree units are defined in which the reduced mass in nitrogen is taken to be unity.

[14]M. H. Cohen, D. A. Goodings, and V. Heine, Proc. Phys. Soc. (London) 73, 811 (1959).

[15]R. K. Nesbet, in Ref. 1, Vol. 9, p. 321.

[16]V. Heine, Czech. J. Phys. 13, B619 (1963).

[17]H. A. Bethe, Phys. Rev. B 138, 804 (1965).

[18]E. Clementi, J. Chem. Phys. 38, 2248 (1963).

[19]L. D. Landau and E. M. Lifshitz, *Quantum Mechanics* (Addison-Wesley, Reading, Mass., 1958), p. 125.

[20]E. Clementi, IBM J. Res. Develop. 9, 2 (1965).

[21]A. Veillard and E. Clementi, J. Chem. Phys. 49, 2415 (1968).

[22]N. C. Dutta and M. Karplus (unpublished).

PHYSICAL REVIEW A VOLUME 6, NUMBER 3 SEPTEMBER 1972

Correlation Energies of Ten-Electron Molecular Systems by a United-Atom Many-Body Perturbation Procedure: H_2O, NH_3, and CH_4†

Taesul Lee and T. P. Das

Department of Physics, State University of New York, Albany, New York 12222

(Received 24 November 1971)

The linked-cluster many-body perturbation theory has been applied to the calculation of the correlation energies of the molecular systems H_2O, NH_3, and CH_4. The Hartree-Fock and correlation energies are obtained separately by combining the contributions from the pertinent diagrams. The calculated Hartree-Fock energies are in satisfactory agreement with the best previous theoretical results. The correlation energies (in a.u.) that we have obtained are −0.338, −0.317, and −0.312 for H_2O, NH_3, and CH_4, respectively. These latter energies are utilized for two purposes. One is to combine them with the total Hartree-Fock energies to obtain the total energies to compare with experiment. Secondly, they are subtracted from the "experimental" total energies to obtain reference Hartree-Fock energies with which to compare the energies from theoretical one-electron calculations.

I. INTRODUCTION

Recently, with advances in computing techniques, accurate variational molecular orbitals approximated as a linear combination of atomic orbitals (LCAOMO) wave functions approaching self-consistent Hartree-Fock character have become available in a number of diatomic molecules.[1] Correlation effects have also been included by variational techniques, using the configuration-interaction (CI) approach.[2] Corresponding calculations in polyatomic molecules involving three, four, and five atoms are much more time consuming, hence relatively few such molecules have been investigated for both HF and correlated wave functions and energies.

In recent work,[3] we have applied the linked-cluster many-body perturbation-theory (LCMBPT) procedure, which has been very successful for properties of atomic systems, to calculate the energy of hydrogen fluoride molecule using as a basis set the eigenfunctions of the corresponding united atom, namely, neon. The result for the energy obtained there agrees very well with experiment and the most detailed CI calculation available.[2] The result of the hydrogen fluoride work indicates that the many-body perturbation approach is certainly comparable in accuracy to the variational two-center method and involves a comparable amount of computational effort. The effort involved in calculating two-center integrals in the latter procedure is substituted by that for calculating

perturbation diagrams resulting from the multipole expansions of the perturbation potential, representing the difference between the one-center and molecular Hamiltonians. Correspondingly, the effort needed to solve the secular equations in the variational method is substituted by the need for evaluating perturbation sums for each diagram over excited states. In addition, the many-body perturbation procedure has a number of attractive features. As has been shown in atomic calculations,[4] the perturbation diagrams give information on various physical effects such as, for example, the role of pair correlation, pair-pair correlation, and three-particle interactions. Secondly, with this procedure, one can separately obtain both the Hartree-Fock one-electron energy as well as the correlation energy. The important point in this respect is that the latter is not evaluated as a difference of large energies, namely, the total and the Hartree-Fock energies, but directly in terms of relatively small numbers, corresponding to the particular diagrams representing correlation effects. In addition, the united-atom model for many-body perturbation calculations has the advantage in terms of computing efforts in that the same basis set of states can be used for a number of isoelectronic molecules. The present paper is concerned with LCMBPT united-atom calculations of the energies of H_2O, NH_3, and CH_4 molecules. In addition to the interest in the energies of these molecules itself, there is interest in the present calculation as it provides a more severe test of the perturbation approach, since the perturbation potential with respect to the neon atom as a reference becomes increasingly stronger in going from HF to CH_4 molecules. Also the results in this series of molecules isoelectronic with neon provide information on the trend of correlation energies in going from the truly one-center-system neon to systems with the electronic distribution extending over increasing numbers of atoms.

In Sec. II we discuss the diagrams and their physical implications, and the process of evaluating them. In Sec. III, the contributions of the various diagrams and results for the net Hartree-Fock, the correlation, and the total energies are presented for the three molecules. The detailed results are compared with those for the isoelectronic systems Ne and HF, and the total energies are compared with experiment. The significance of the results will be discussed and comparison will be made with other available calculations. Finally, conclusions are listed in Sec. IV.

II. THEORY AND DIAGRAMS

The nonrelativistic Hamiltonian for a ten-electron molecular system XH_n with fixed nuclear coordinates is given by (in a.u.)

$$\mathcal{H}=\sum_{i=1}^{10}\left(-\tfrac{1}{2}\nabla_i^2-\frac{10-n}{r_i}-\sum_{\alpha=1}^{n}\frac{1}{r_{\alpha i}}\right)+\sum_{i>j}v_{ij}+\left(\frac{(10-n)n}{R_{XH}}+\frac{n(n-1)}{2R_{HH}}\right). \quad (1)$$

In Eq. (1), $\vec{r}_i$ and $\vec{r}_{\alpha i}$ are electronic radius vectors measured with respect to the X and the αth H nucleus, respectively, as the origin, and v_{ij} is the electron-electron interaction between two electrons i and j. The summation over α extends from 1 to n, with $n=1, 2, 3$, and 4 for HF, H_2O, NH_3, and CH_4. R_{XH} and R_{HH} in the last term of Eq. (1) represent the internuclear separations.[5] Since the last term in Eq. (1) is taken to be a constant, this term will be omitted until we discuss the final results for the total energy of XH_n. For the present analysis, it is convenient to rewrite Eq. (1) in the form

$$\mathcal{H}=\sum_{i=1}^{10}\left(-\tfrac{1}{2}\nabla_i^2-\frac{10}{r_i}\right)+\sum_{i>j}v_{ij}+\sum_{i,\alpha}\left(\frac{1}{r_i}-\frac{1}{r_{\alpha i}}\right)$$

$$=\mathcal{H}_0+\left(\sum_{i>j}v_{ij}-\sum_{i=1}^{10}V_i^{N-1}\right)+\sum_{i,\alpha}\left(\frac{1}{r_i}-\frac{1}{r_{\alpha i}}\right),$$

where $\mathcal{H}_0$ is the zeroth-order Hamiltonian given by

$$\mathcal{H}_0=\sum\left(-\tfrac{1}{2}\nabla_i^2-10/r_i+V_i^{N-1}\right) \quad (2)$$

and is the V^{N-1} Hamiltonian[6] for the neon atom[4] which is also the pertinent united atom for the systems discussed in the present investigation. This choice of $\mathcal{H}_0$ gives rise to two terms $\mathcal{H}_1'$ and $\mathcal{H}_2'$ to be treated as small perturbations. We define $\mathcal{H}_1'$ and $\mathcal{H}_2'$ as follows:

$$\mathcal{H}'=\mathcal{H}_1'+\mathcal{H}_2'=\mathcal{H}-\mathcal{H}_0,$$
$$\mathcal{H}_1'=\sum_{i>j}v_{ij}-\sum_i V_i^{N-1},\qquad \mathcal{H}_2'=\sum_{i,\alpha}\left(\frac{1}{r_i}-\frac{1}{r_{\alpha i}}\right). \quad (3)$$

In Eqs. (3), $\mathcal{H}_1'$ represents the usual perturbation due to the difference between the actual electron-electron interactions and the averaged interaction represented by the V^{N-1} potential. $\mathcal{H}_2'$ represents the perturbation due to the difference in the nuclear interactions in the molecule and the united atom. It is this perturbation that restores the multicenter nature of the molecules which is absent in the united-atom Hamiltonian $\mathcal{H}_0$. It is thus appropriate to refer to $\mathcal{H}_2'$ as the molecular deformation potential. The complete set of basis states associated with $\mathcal{H}_0$, namely, the neon-atom basis set, was the same as that used in earlier work on neon.[4]

Since the $\mathcal{H}_0$ basis states are centered about the X nucleus, it is appropriate to expand $1/r_{\alpha i}$ about the same center, namely,

$$\mathcal{H}_2'=\sum_i\left(\frac{1}{r_i}-\sum_{l=0}^{\infty}\frac{4\pi}{2l+1}\frac{r_<^l}{r_>^{l+1}}\right.$$

$$\times \sum_{m=-l}^{l} [\, Y_{lm}(\Omega_i) \sum_{\alpha=1}^{n} Y^*_{lm}(\Omega_\alpha)] \Big) \ ,$$

where $r_<$ (or $r_>$) is the lesser (or greater) of r_i and R_{XH}. For purposes of our calculation, it is convenient to reexpress $\mathcal{H}_2'$ in the form

$$\mathcal{H}_2' = \sum_{l=0}^{\infty} \gamma_l \ ;$$

where for $l=0$,

$$\gamma_0 = n \sum_i \left(\frac{1}{r_i} - \frac{1}{r_>} \right) = n \sum \left(\frac{1}{r_i} - \frac{1}{R_{XH}} \right) \quad \text{for } r_i \leqq R_{XH}$$

$$= 0 \quad \text{for } r_i \geqq R_{XH} \ ,$$

and for $l \neq 0$,

$$\gamma_l = - \sum_i \frac{4\pi}{2l+1} \frac{r_<^l}{r_<^{l+1}} \sum_{m=-l}^{l} [\, Y_{lm}(\Omega_i) \sum_{\alpha=1}^{n} Y^*_{lm}(\Omega_\alpha)] \ .$$

The total energy of the system is given by

$$E_{\text{tot}} = E_0 + \frac{(10-n)n}{R_{XH}} + \frac{n(n-1)}{2R_{HH}} + \sum \langle \Phi_0 \mid \mathcal{H}' \left(\frac{1}{E_0 - \mathcal{H}_0} \mathcal{H}' \right)^n \mid \Phi_0 \rangle_L \ , \quad (4)$$

where the first term on the right-hand side represents the sum of the one-electron orbital energies in the neon V^{N-1} potential. The next term represents the repulsive energy between the central nucleus and the protons in the molecule. The third term represents the proton-proton repulsion, all proton-proton distances within a particular molecule being equal due to symmetry. The fourth term is the usual linked-cluster perturbation expansion[7] to the energy. Since $\mathcal{H}'$ is the sum of $\mathcal{H}_1'$ and $\mathcal{H}_2'$, one can obtain sets of diagrams involving $\mathcal{H}_1'$ vertices only, $\mathcal{H}_2'$ vertices only, and combinations of $\mathcal{H}_1'$ and $\mathcal{H}_2'$ vertices.

The diagrams involving only $\mathcal{H}_1'$ vertices are identical to the energy diagrams in the neon atom. The rest of the diagrams represent the polarization effect due to the perturbation $\mathcal{H}_2'$ which converts the neon atom into the molecule in question. In describing and listing the diagrams we have felt it meaningful to divide the diagrams into two broad classes, according to whether they are one-electron diagrams or correlation- (many-electron) energy diagrams. Topologically, those diagrams which always involve only one electron excited at a time represent one-electron effects, while diagrams which involve more than one-electron excited at any instant of time[8] represent correlation effects. There are some exceptions to this rule to be discussed later in this section. This permits us to obtain the Hartree-Fock and correlation energy separately. Within each of these two classes, we

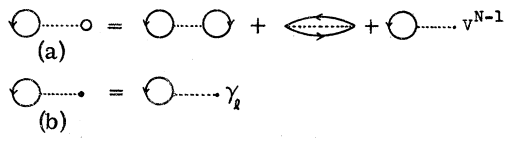

FIG. 1. (a) Hartree-Fock zero grand order energy diagram. (b) Hartree-Fock first grand order energy diagram.

have separated the diagrams according to the number of orders of $\mathcal{H}_2'$ that are involved.

Since we shall be combining into groups all diagrams which involve the same number of order in $\mathcal{H}_2'$ and all order in $\mathcal{H}_1'$ wherever possible and necessary, it is helpful to use the term grand order to characterize such groups of diagrams. Thus a group referring to grand order n will have, for all its diagrams, n $\mathcal{H}_2'$ vertices and any number of vertices corresponding to $\mathcal{H}_1'$.

Considering the Hartree-Fock diagrams first, in zero grand order, we have one group of diagrams in Fig. 1(a) which as usual provides the correction to the sum of the orbital energies in neon owing to the fact that such a sum counts the Coulomb and exchange energies twice.

For the first grand order, we have the diagrams shown in Fig. 1(b). This diagram represents the net first-order correction due to the deformation potential.

Under the second grand order, we have the group of diagrams listed in Fig. 2. These diagrams are analogous to the polarizability diagrams of neon[9] except that our deformation potential now has all orders in γ_l simultaneously, instead of the one particular l value that one considers for the calculation of a particular multipole polarizability. In general, the two γ vertices can refer to different l values in all the diagrams in Fig. 2 except for the first one where the l values at the two vertices have to be equal from angular momentum considerations. However, since neon has spherical symmetry, in fact, except for a few exceptions, all the diagrams involve two vertices with same l. The first diagram in Fig. 2 represents the direct effect on the neon orbitals of two orders in the deformation potential. In this diagram, each neon orbital is individually polarized by the deformation potential and the polarized orbital interacts with the latter just as in the polarizability problem. The diagrams 2(b)–2(e) represent the corrections to diagram 2(a) due to the interaction between the electronic states while they are subject to the deformation perturbation. Thus these diagrams essentially correspond to the self-consistency correction terms in the method-A procedure for polarizability calculations discussed by Langhoff, Karplus, and Hurst.[10] It should be re-

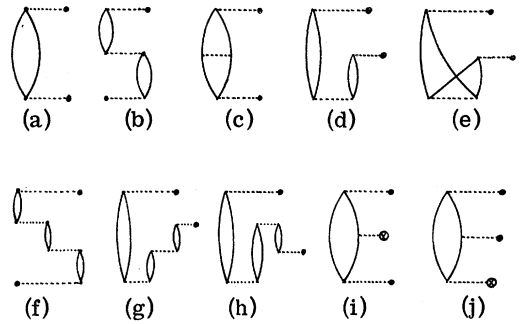

FIG. 2. Typical second grand order Hartree-Fock energy diagrams.

marked that although diagrams 2(d) and 2(e) appear to involve two particles excited simultaneously, in fact, as shown by Langhoff, Karplus, and Hurst, they represent perturbation terms in the energy which arise from taking a determinantal wave function in the perturbed state. These diagrams have therefore to be grouped with one-electron diagrams. The values of the diagrams 2(b)–2(e) show that they do provide substantial shielding corrections to the diagram 2(a). The diagram 2(c) is the exchange version of 2(b). We have included the effects of these shieldings to all orders in $\mathcal{H}_2'$, both within each diagram type [for example, 2(f)] as well as for combinations of the various types of vertices [for example, 2(g) and 2(h)] in the four different vertices shown in Figs. 2(b)–2(e). This was accomplished by the usual geometric-series approximation procedure[11] involving examinations of diagrams of successively higher orders in electron-electron vertices.

There are some additional one-particle excitation diagrams in each grand order involving the 1*s* hole state of neon, which are small compared to those discussed so far. These diagrams, examples of which for second grand order are shown in Figs. 2(i) and 2(j), are analogous to corresponding ones in neon and result from the use of the V^{N-1} potential, and take account of the small difference between the true Hartree-Fock energy and the one-electron energy in a V^{N-1} potential. We have included all the contributions from these diagrams in the present calculation.

In describing higher g order diagrams, it is necessary for purposes of brevity of notation to introduce the interaction vertex in Fig. 3, which shows a screened deformation potential vertex inserted on a hole line. The solid horizontal bar will be used to denote this screened vertex in contrast to the dotted bar in Fig. 1(b) which represents the bare $\mathcal{H}_2'$ interaction vertex. It should be remarked that in Fig. 3, the right-hand side should involve an infinite series representing the contribution from all orders in electron-electron interactions. This would mean adding successive orders of lenses in Fig. 3(b) and exchange counterparts in Fig. 2(c) and combinations of both to all orders. Also either or both of the dotted lines in Fig. 3(a) at the extremities of the diagram can be replaced by solid lines with the same meaning as that for the middle line. The sum total of the third grand order diagrams including shielding effects is represented in a compact form by the diagram in Fig. 4(a). The middle interaction line (solid line) indicates the sum of two diagrams, one with the interaction line on the hole side, and the other with that on the particle side. This then gives a convenient notation for representing the composite of all diagrams representing higher grand orders as indicated for fourth order in Figs. 4(b)–4(d). In our present work, we have evaluated the Hartree-Fock diagrams through fourth grand orders.

For the correlation energies, the typical diagrams are shown in Fig. 5. The zero grand order diagrams shown in Figs. 5(a)–5(d) correspond to those for the neon atom.[5] The first two diagrams represent the pair-correlation energies which gave about 106% of the neon correlation energy. The rest of the correlation-energy diagrams in neon accounted for the balance of 6% almost all of which was accounted for the pair-pair correlation-energy diagrams in Figs. 5(c) and 5(d). The first grand order diagrams presented in Figs. 5(e)–5(h) form two distinct subclasses. The first subclass, typified by Figs. 5(e) and 5(f), represents the influence of the deformation potential on the neon correlation-energy diagrams. Here the middle horizontal (solid) line can be attached to any of the two hole lines and two particle lines in the diagram. Besides these two diagrams, we have also included the diagrams that result from attaching the $\mathcal{H}_2'$ line to the pair-pair correlation-energy diagrams in Figs. 5(c)–5(d). The second subclass of the first grand order diagrams involving Figs. 5(g) and 5(h) is typical of the molecular system and cannot be obtained by attaching an $\mathcal{H}_2'$ vertex to any of the neon correlation-energy diagrams. Physically these diagrams represent the influence of many-body interactions among electrons on the response of individual electrons to the deformation potential. In this respect, they are similar to the diagrams 2(b)–

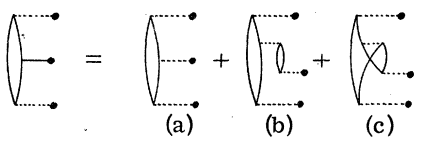

FIG. 3. Screened-deformation-potential vertex inserted in a hole line.

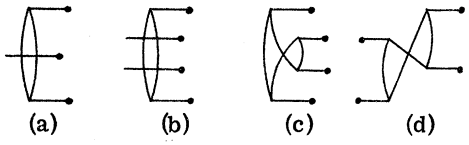

FIG. 4. Third and fourth grand order diagrams in compact forms.

2(e) which describe the role of one-electron consistency effect on the perturbation due to the deformation potential. Diagrams such as 5(i)–5(k) represent the combined influence of the correlation and consistency effects on the perturbation of the one-electron states by the deformation potential. The last two diagrams in Fig. 5 represent typical third grand order correlation-energy diagrams.

III. RESULTS AND DISCUSSION

In Table I, we have listed our calculated contributions from various grand orders for both the Hartree-Fock and correlation energies as well as the total energies for all three molecules studied in this work. For purposes of comparison, corresponding contributions for HF molecule are also included from earlier work.[3] The last row gives the experimental values of the nonrelativistic total energies. The nonrelativistic total experimental energies which are the pertinent ones to use here for purposes of comparison can be obtained by the same procedure that was adopted for HF molecule.

TABLE I. Summary of the results on the Hartree-Fock, correlation, and total energies.

Grand orders	HF	H_2O	NH_3	CH_4
		Hartree-Fock energy[a]		
0	−123.356	−119.362	−116.578	−114.489
1	25.398	51.279	77.745	105.221
2	−1.797	−7.214	−15.854	−26.734
3	−0.291	−0.731	−1.618	−4.304
4	0.010	0.030	0.154	0.485
$E_{Ha.}$	−100.036 ± 0.1	−75.998 ± 0.15	−56.151 ± 0.2	−39.821 ± 0.4
		Correlation energy		
0	−0.3878	−0.3878	−0.3878	−0.3878
1	0.0319	0.0576	0.0873	0.1049
2	−0.0013	−0.0053	−0.0119	−0.0211
3	−0.0005	−0.0020	−0.0046	−0.0081
E_{corr}	−0.3577 ± 0.01	−0.3375 ± 0.01	−0.3170 ± 0.01	−0.3121 ± 0.01
E_{tot}	−100.394[b] ± 0.1	−76.336 ± 0.15	−56.468 ± 0.2	−40.133 ± 0.4
E_{expt}	−100.4535	−76.4347	−56.5601	−40.5100

[a]Atomic units are used (1 a.u. of energy = 27.2097 eV).
[b]This number is slightly different from that quoted in Ref. 3 due to somewhat different approximation involved in summing over higher-order diagrams.

This procedure consists of combining experimental dissociation energy data[12] for the molecule with experimental total energies for the separated atoms using ionization data[13] for the latter and making corrections for relativistic effects[14] to obtain the nonrelativistic energy.

Before further discussion about the results in Table I, we would like to analyze some of the contributions from which the various grand orders are composed. The zero grand order contributions are a result of combination of neon Hartree-Fock energy and the nuclear repulsion energies in these molecules. The first grand order contribution arises primarily from Fig. 1(b) and includes small corrections due to screening effects corresponding to the replacement of the dotted line in Fig. 1(b) by the solid line in Fig. 3, as discussed in Sec. II. The second grand order results broken down in Table II illustrate the substantial shielding effects that result from electron-electron interactions. In Table II, the first row represents the contribution from diagram 2(a) describing the second-order polarizations of the individual orbitals by the deformation potential. The next four rows give the contributions from diagrams 2(b)–2(e) which represent the influence of electron-electron interactions. The number for diagram 2(b) includes the effects of diagrams such as 2(f) and its higher-order counterparts obtained through the geometric-series approximation. Similarly the contribution listed for diagram 2(d) includes the contributions from diagrams 2(g) and 2(h) and their higher-order counterparts. It should be pointed out that diagrams such as 2(f)–2(h) have companions of the same order involving exchange and different time orderings of the various vertices. All these diagrams were included in the analysis. Small contributions from diagrams 2(i) and 2(j) are also included in the numbers quoted for 2(c) and 2(e), respectively. The net screening contribution

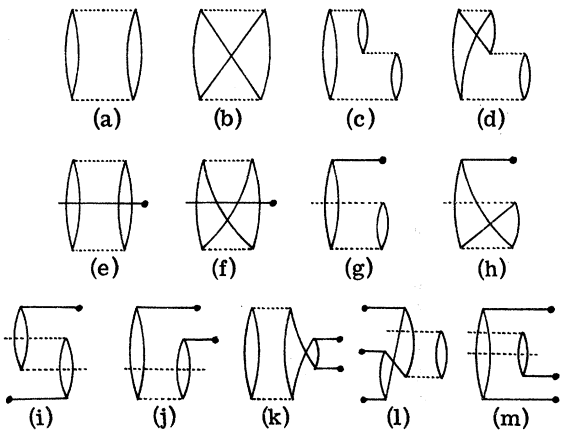

FIG. 5. Correlation-energy diagrams.

TABLE II. Contributions from the second grand order Hartree-Fock energy diagrams.

Diagram	HF	H_2O	NH_3	CH_4
2(a)	−2.845	−11.391	−25.660	−45.999
2(b)	0.714	3.099	7.089	12.564
2(c)	−0.130	−0.543	−1.289	−2.083
2(d)	0.486	1.989	4.543	9.951
2(e)	−0.022	−0.368	−0.537	−1.167
Total	−1.797	−7.214	−15.854	−26.734

due to electron-electron interactions has been found to be about 40% of the bare diagram 2(a). In the third grand order, there are a number of diagrams as mentioned earlier, the composite of which is represented by Fig. 4(a). In evaluating these diagrams, one has to take into account the screening that accompanies all three γ vertices. Percentagewise, the screening is now more pronounced than for the second grand order, being about 75% of the bare diagram consisting of three γ vertices (dotted line). This stronger cancellation helps the convergence in orders. In the fourth grand order, from the diagram represented by Fig. 4(b) which is a simple extension of the diagram 4(a) with one additional screened γ vertex, there is a small negative contribution. However, one now has a new topological arrangement of vertices represented by Fig. 4(c) and its various counterparts, a typical example being that in Fig. 4(d). These diagrams produce positive contributions larger in magnitude than the negative contribution from Fig. 4(b).

Table III gives a breakdown of the contributions to diagram 2(a) from hole states $1s$, $2s$, and $2p$. For each of these states, contributions from various particle states of different l are listed to illustrate the l convergence of this diagram. The contributions from s-particle states for $1s$ and $2s$ and p-particle states for $2p$ result from vertices associated with γ_0 and are seen to be of comparable magnitude with $2p$ the largest followed by $1s$. The p-particle contributions for the s-hole states and s- and d-particle contributions for the p-hole state arise from γ_1 vertices in diagram 2(a) and are indicative of the dipole polarizabilities of the three types of hole states. It should be remarked that the $2p \rightarrow p$ excitation could also be brought about by a combination of γ_2 vertices instead of two γ_0 vertices. The contribution from the former was found to be about 1% of the latter. A similar observation applies to the ratio of (γ_3, γ_3) to (γ_1, γ_1) vertex-combination contributions for $2p \rightarrow d$ excitations. An examination of the contributions from the various l states as listed in Table III for all four molecules indicates that satisfactory convergence has been achieved in terms of the influence of the various multipoles γ_l.

TABLE III. Contributions to the diagram 2(a) from various l-excitations.

n	k	HF	H_2O	NH_3	CH_4
$1s$	s	−0.712	−2.911	−6.548	−11.638
	p	−0.0	−0.0	−0.0	−0.0
$2s$	s	−0.464	−1.945	−4.396	−7.858
	p	−0.002	−0.003	−0.002	...
	d	−0.005	−0.005	−0.003	...
	f	−0.002	−0.003	−0.002	−0.006
$2p$	s	−0.008	−0.012	−0.010	...
	p	−1.579	−6.403	−14.623	−26.467
	d	−0.063	−0.098	−0.070	−0.030
	f	−0.010	−0.011	−0.006	...
Total		−2.845	−11.391	−25.660	−45.999

The contributions from the zero grand order correlation-energy diagrams in Figs. 5(a)–5(d) listed in Table I were taken from the calculation on neon. Table IV lists the contributions from correlation-energy diagrams in Figs. 5(e)–5(h). As explained in Sec. II, diagrams 5(e) and 5(f) are the composites of four sets of diagrams corresponding to the solid line attached to the two holes and two particle lines in the diagram. The solid line as usual represents a screened vertex which is illustrated in Fig. 3. The numbers in the first row in Table IV represent the net contribution from the diagram 5(e) due to vertices of the type shown in Fig. 3(a). The second row is the sum of the corresponding contributions from vertices of the types shown in Figs. 3(b) and 3(c) and their higher-order variations. The next two rows are the counterparts of the first two rows for the diagram 5(f). Again an examination of the relative magnitudes of the second-row contributions with respect to the first row and of the fourth row with respect to the third row indicates a screening effect from the electron-electron interactions comparable to that for Fig. 2, namely, about 35%. The diagrams 5(g) and

TABLE IV. Contributions from the first grand order correlation-energy diagrams.

Diagram	HF	H_2O	NH_3	CH_4
5(e)	−0.0048	−0.0089	−0.0153	−0.0193
	0.0017	0.0028	0.0061	0.0082
5(f)	0.0026	0.0053	0.0078	0.0095
	−0.0009	−0.0020	−0.0029	−0.0035
5(g)	0.0296	0.0538	0.0815	0.0980
5(h)	0.0037	0.0066	0.0101	0.0220
Total	0.0319	0.0576	0.0873	0.1049

TABLE V. Summary of earlier works on energies for ten-electron systems.

Reference	HF	H_2O	NH_3	CH_4
One-electron				
One-center				
15	−100.005	−75.922	−55.972	−39.866
16			−56.081	
17	−99.827	−75.934	−56.188	−39.971
Present calculation	−100.04	−76.00	−56.15	−39.82
E^*_{HF}[a]	−100.096	−76.097	−56.243	−40.198
Multicenter				
18		−76.034	−56.201	−40.198
19		−76.066[b]		
1	−100.07			
20			−56.185	
Many-electron				
One-center				
21		−76.48+0.07		
Presnet calculation	−100.40 +0.1	−76.33 +0.15	−56.47 +0.2	−40.13 +0.4
Multicenter				
2	−100.356			
22		−76.148(GTO)		
22		−76.145(STO)		
23		−76.144	−56.288	−40.314
E_{expt}	−100.454	−76.435	−56.560	−40.510

[a]The reference HF energy defined in the text.

[b]This result was obtained from a STO basis set. Neumann and Moskowitz obtained −76.059 from a GTO basis set [D. Neumann and J. W. Moskowitz, J. Chem. Phys. 49, 2056 (1968)].

5(h) make the contributions listed in the fifth and sixth rows of Table IV. These diagrams, as mentioned earlier, are typical of the molecular system and cannot be related to the united-atom diagrams. They make substantially larger contributions than Figs. 5(e) and 5(f). In view of this, in the higher grand orders, only the diagrams 5(i)–5(m) which result from additional perturbations of diagrams 5(g) and 5(h) were included. The third grand order contributions are estimated from the diagrams 5(l) and 5(m).

Returning to Table I, we like to comment first on the error limits that we have ascribed to the Hartree-Fock, correlation, and total-energy results. Since the fourth grand order diagrams have not been exhaustively studied, we expect conservatively an error limit from this estimation of about 50% of the results that we have listed under the fourth grand order contributions. An additional 10% of the fourth grand order contribution was also added to the error limit to reflect possible contributions from higher grand orders. Additionally, an error limit of 0.1 a.u. has been added as a conservative estimate of the accuracy of the numerical procedures involved in evaluating the diagrams. This limit is much larger than what we have estimated in earlier energy calculations of atoms,[4] because the sizes of the diagrams involved here are much larger. For the correlation energies, the main error limits are set by those in the neon correlation-energy calculation. These error limits dominate the small range of additional errors that result from the fact that the third grand order contribution is of the nature of an estimate and higher grand orders are neglected. The error limits for the total energies are determined by the corresponding limits for the Hartree-Fock energies, since the error limits of the correlation energies are much smaller.

Our calculated total energies for HF, water, and ammonia are in satisfactory agreement with the experimental results. For methane, the agreement is somewhat less satisfactory. This trend is expected, since the perturbation potential $\mathcal{H}_2'$ gets increasingly stronger as one goes from HF to methane, leading to relatively larger contributions from fourth and higher grand orders. We shall discuss later in this section possibilities for improving the Hartree-Fock results.

The correlation energies ΔE_{corr} are seen to vary very little in going from neon ($\Delta E_{corr} = -0.38914$) to methane. This is a consequence of the fact that the over-all volume over which the electrons are distributed does not change drastically over the entire series of these five isoelectronic systems. Whatever variation there is in ΔE_{corr}, can be physically understood as follows. The pair-correlation energy reflects the tendency of electrons to stay further apart beyond what is expected through the Hartree-Fock potential. The tendency to stay apart is stronger when the electrons are confined to a smaller volume and the average pair separation is expected to increase significantly in going from neon to HF, since the electrons now spend part of the time on two separate atoms. This explains the observed decrease in ΔE_{corr}. A further increase in the average pair separation and corresponding decrease in correlation energy is expected in going from HF to the five-atom-system methane as is observed from Table I, although the decrease is less significant than in going from neon to HF, where the largest relative change in pair separation is expected.

Finally we would like to compare our Hartree-Fock and total-energy results with those of earlier calculations. A number of one-electron calculations have been performed on these molecules. In Table V, we have listed the results of only a selected number of one-electron calculations which we felt were the most extensive of the available ones. The number of many-body calculations available is much fewer than one-electron ones. We have listed all the available results in this case. Included in the table are our Hartree-Fock and total-energy results taken from Table I as well as the experimental total energies and reference Hartree-Fock ener-

gies. The latter are obtained by subtracting our calculated correlation energies from the experimental total energies. This is the reverse of what is usually done in atomic and molecular calculations, where one subtracts the best Hartree-Fock energy from the experimental total energy to obtain a correlation energy. With the LCMBPT procedure, it is however possible to obtain the correlation energy as a separate entity from an estimation of the correlation-energy diagrams. In the present work, the correlation energy is obtained with an accuracy comparable to the experimental total energy and therefore it is justifiable to use the difference between the experimental total energy and the calculated correlation energy as a reference to compare with theoretical Hartree-Fock calculations.

Considering the one-electron energies first, the earlier calculations are grouped under two broad categories—one center and multicenter. Among the one-center calculations, there is first the method used by Moccia[15] which utilizes a variational procedure to obtain one-electron wave functions for the molecule using a linear combination of Slater-type orbitals (STO) centered on the heavy atom. Joshi's calculation[16] for ammonia is of the same type except that he used the larger basis set of 25 STO (instead of Moccia's 21) and optimized exponents in the variational calculation. Also he utilized STO's with l up to 5 while Moccia had gone up to $l=3$. The other type of one-center calculation that has been performed is by Kim and Parr[17] who utilized the so-called "molecular puff" Hamiltonian for the zeroth-order approximation. This potential can be best described as a combination of the neon-atom potential and γ_0 term in $\mathcal{H}_2'$ except that the Coulomb and exchange contributions to the one-electron potential were determined self-consistently instead of using neon orbitals for this purpose as we have done. Using their zero-order orbitals, Kim and Parr obtained the energy up to second order in the γ_l terms for $l=1$ to $l=10$. In order to simplify their computational procedure, Kim and Parr utilized single-exponent nodeless STO with optimized exponents for the zero-order wave functions. The use of orbitals of this form allowed them to obtain the perturbation due to γ_l in the one-electron wave functions, by analytic solution of the corresponding first-order equations.

The multicenter one-electron results which are listed in Table V were all obtained through variational self-consistent-field (SCF) LCAOMO calculations. The calculations[18–20] on water, ammonia, and methane were performed using Gaussian orbitals, while Cade and Huo's calculation[1] on HF utilized a linear combination of STO's.

In the case of HF molecule, our one-center perturbation calculation gave a lower one-electron energy than the other two one-center calculations. The two-center SCF calculation by Cade and Huo, however, gives a slightly lower energy than our result and is only about 0.023 a.u. higher than the experimental Hartree-Fock energy. For water, again our calculated one-electron energy is lower than these from the other two one-electron one-center calculations. The two SCF LCAOMO results, however, are lower than ours by about 0.03 and 0.06 a.u., respectively, the lower of these being about 0.038 a.u. higher than the reference Hartree-Fock result. In the case of ammonia, our calculated one-electron energy is lower than both Moccia[15] and Joshi,[16] but a little higher than Kim and Parr.[17] In Kim and Parr's calculation, the perturbation effect of $\mathcal{H}_2'$ is handled somewhat better than in our treatment because they absorbed γ_0 in the zero-order Hamiltonian. On the other hand, the accuracy of their results suffers somewhat from the use of the rather simplified one-exponent variational functions. For ammonia, the perturbation effect is much stronger than in water and HF, and their formulation in terms of the weaker perturbation Hamiltonian has a definite advantage over our calculation and leads to an energy lower than ours. This feature is even more marked in the case of methane where the perturbation Hamiltonian in our treatment is relatively strong and makes our Hartree-Fock energy about 0.15 a.u. higher than Kim and Parr. For both ammonia and methane, the multicenter SCF calculations give lower energies than the best one-center results. For ammonia, the best multicenter one-electron energy is only 0.02 a.u. higher than the reference Hartree-Fock energy. For methane, there seems to be almost exact agreement between the lowest theoretical Hartree-Fock energy and the reference Hartree-Fock energy.

As regards other many-body calculations, these can also be divided into one-center and multicenter categories. The only other one-center calculation beside ours is that on water by Miller and Kelly[21] who have also utilized the LCMBPT approach. However, instead of using the neon-atom potential as the starting point as we do, they use for their zero-order Hamiltonian the V^{N-1} potential corresponding to neutral oxygen. Thus their perturbation potential consists of contributions from the two hydrogen atoms with a substantial cancellation between the matrix elements involving the potential due to the protons and those due to the accompanying electrons. This cancellation is analogous to the cancellation that we have found in each grand order between diagrams involving the bare γ_l vertex and those involving in addition, the effects of electron-electron interaction vertices. The other many-body results listed in Table V were obtained through the variational CI procedure using the occupied and unoccupied orbitals obtained

from SCF LCAOMO calculations to create determinantal wave functions corresponding to the various configurations utilized in the calculations. For HF, the result of our calculation for the total energy is lower than the available CI results. The experimental total energy lies within the limits of error of our results. For water, our calculated total energy is lower than the results from the available CI calculations[22,23] listed in Table V. The experimental total energy lies within the range of the error of our calculation. It is interesting that while our calculated total energy is slightly higher than experiment, that of Miller and Kelly[21] is slightly lower. Since many-body perturbation calculations do not utilize the variation principle, there is no lower bound on the results and hence one can obtain an energy lower than experiment by the LCMBPT procedure. For ammonia, our total energy is again lower than the available results from CI calculations.[23] This is interesting, since our calculated Hartree-Fock energy was higher than the SCF molecular orbital results listed in Table V. The relatively high total energy from CI calculations could be interpreted as indicating that all of the correlation energy has not been included in the CI calculations.

For the methane molecule, our total energy is higher than the available CI results.[23] We feel that this is a consequence of the difference between our calculated Hartree-Fock energy and the reference Hartree-Fock energy pointed out earlier. The CI result is about 0.186 a.u. higher than experiment, which may again indicated that the correlation effects have not been completely incorporated in the CI calculations.

IV. CONCLUSIONS

Thus our many-body perturbation calculation using the united-atom potential as the starting point gives results comparable in accuracy with other many-body calculations for HF, H_2O, and NH_3. In the cases of HF and NH_3, our results for the total energy are numerically in better agreement with experiment than other available theoretical results. For methane, our procedure is somewhat less successful than for the other three molecules due to the greater strength of the perturbation $\mathcal{H}_2'$. In fact, it is mainly the Hartree-Fock energy whose accuracy as reflected by the larger range of error quoted in Table I, is influenced by the slower convergence of the perturbation results. To improve upon this convergence, one would have to use an $\mathcal{H}_0$ which makes the perturbation Hamiltonian $\mathcal{H}_2'$ weaker than the present choice. One such possible choice for $\mathcal{H}_0$ would be to include γ_0 in $\mathcal{H}_0$ but with the occupied orbitals (hole states) obtained self-consistently. This choice is thus similar to that of Kim and Parr. The perturbation diagrams would no longer involve the relatively strong term γ_0 and would therefore lead to better convergence. However, such a calculation would be more time consuming, since it would require a separate basis set of states for each molecule. Finally, it is expected that the application of the united-atom LCMBPT procedure to heavier molecules of the family such as those based on the argon, krypton, and xenon united atoms should lead to even better convergence than here, since the deformation potential is expected to be relatively weaker compared to $\mathcal{H}_0$.

†Work supported by the National Science Foundation.

[1]Paul E. Cade and Winifred M. Huo, J. Chem. Phys. 47, 614 (1967).

[2]Charles F. Bender and Ernest R. Davidson, Phys. Rev. 183, 23 (1969).

[3]T. Lee, N. C. Dutta, and T. P. Das, Phys. Rev. Letters 25, 204 (1970).

[4]Taesul Lee, N. C. Dutta, and T. P. Das, Phys. Rev. A 4, 1410 (1971).

[5]We have used the experimental values of R_{HH} and R_{XH} in our calculations. See Ref. 15.

[6]H. P. Kelly, Phys. Rev. 136, B896 (1964).

[7]J. Goldstone, Proc. Roy. Soc. (London) A239, 267 (1957).

[8]For the sake of clarity, it should be emphasized that those diagrams which involve both one-electron and many-electron excitations also represent correlation effects.

[9]C. Matsubara, N. C. Dutta, T. Ishihara, and T. P. Das, Phys. Rev. A 1, 561 (1970).

[10]P. W. Langhoff, M. Karplus, and R. P. Hurst, J. Chem. Phys. 44, 505 (1966).

[11]H. P. Kelly, Phys. Rev. 131, 684 (1963).

[12]B. deB. Darwent, National Bureau of Standards Report No. NSRDS-NBS 31 (unpublished).

[13]Charles W. Scherr, Jeremiah N. Silverman, and F. A. Matsen, Phys. Rev. 127, 830 (1962).

[14]H. Hartmann and E. Clementi, Phys. Rev. 133, A1295 (1964); A. Veillard and E. Clementi, J. Chem. Phys. 49, 2415 (1968).

[15]Roberto Moccia, J. Chem. Phys. 40, 2164; 40, 2176 (1964); 40, 2186 (1964).

[16]B. D. Joshi, J. Chem. Phys. 43, 540 (1965).

[17]Hojing Kim and Robert G. Parr, J. Chem. Phys. 47, 3071 (1968).

[18]C. D. Ritchie and H. F. King, J. Chem. Phys. 47, 564 (1967).

[19]T. H. Dunning, R. M. Pitzer, and S. Aung (private communication). See also, R. M. Pitzer and T. H. Dunning, Bull. Am. Phys. Soc. 16, 309 (1971).

[20]R. G. Body, D. S. McClure, and E. Clementi, J. Chem. Phys. 49, 4916 (1968).

[21]John H. Miller and Hugh P. Kelly, Phys. Rev. Letters 26, 679 (1971).

[22]R. P. Hosteny, R. R. Gilman, T. H. Dunning, Jr., A. Pippano, and I. Shavitt, Chem. Phys. Letters 7, 325 (1970).

[23]P. F. Franchini, R. Moccia, and M. Zandomeneghi, Intern. J. Quant. Chem. 4, 487 (1970).